



Published in final edited form as:

Calcif Tissue Int. 2012 September ; 91(3): 215–224. doi:10.1007/s00223-012-9628-z.

Deletion of Cx43 from osteocytes results in defective bone material properties but does not decrease extrinsic strength in cortical bone

Nicoletta Bivi¹, Mark T. Nelson², Meghan E. Faillace^{3,4}, Jiliang Li², Lisa M. Miller^{3,4}, and Lilian I. Plotkin^{1,*}

¹Dept. Anatomy & Cell Biology, Indiana University School of Medicine, Indianapolis, IN

²Department of Biology, Indiana University Purdue University Indianapolis

³National Synchrotron Light Source, Brookhaven National Laboratory, Upton, NY

⁴Dept. Biomedical Engineering, Stony Brook University, Stony Brook, NY

Abstract

Deletion of connexin (Cx) 43 from osteoblasts and osteocytes (OCN-Cre;Cx43^{fl/-} mice) or from osteocytes only (DMP1-8kb-Cre;Cx43^{fl/fl} mice) results in increased cortical, but not cancellous, osteocyte apoptosis and widening of the femoral midshaft without changes in cortical thickness. Despite the consequent larger moment of inertia, stiffness and ultimate load, measures of mechanical strength assessed by 3-point bending, are not higher in either model of Cx43 deficiency, due to reduced Young's modulus, a measure of the stiffness of the material per unit of area. In OCN-Cre;Cx43^{fl/-} mice, this was accompanied by a reduced ratio of nonreducible/reducible collagen cross-links as assessed by Fourier Transformed Infrared Imaging (FTIRI) in the femoral diaphysis. On the other hand, DMP1-8kb-Cre;Cx43^{fl/fl} mice did not show a significant reduction in collagen maturation in the same skeletal site, but a small decrease in mineralization was detected by FTIRI. Remarkably, both osteoblastic and osteocytic cells lacking Cx43 expressed lower mRNA levels of lysyl oxidase, a crucial enzyme involved in collagen maturation. These findings suggest that Cx43 expression in osteoblasts is involved in maintaining the quality of the bone matrix in cortical bone through the maturation of collagen cross-links. Osteocytic Cx43 expression is important also to maintain the stiffness of the bone material, where a Cx43 deficiency results in a local reduction in mineralization, possibly due to osteocyte apoptosis.

Keywords

connexin 43; young's modulus; FTIR; osteocyte; osteoblast; Lox

Introduction

Bone tissue homeostasis is guaranteed by intercellular communication among osteoclasts, osteoblasts and osteocytes. Important mediators of this function are gap junctions, channels that allow coupling between neighboring cells through the passage of small molecules [20]. The most abundant gap junction protein in osteoblastic cells is connexin 43 (Cx43) [11]. Gap junctions result from the juxtaposition of two hexameric hemichannels formed by Cx43, one contributed by each coupled cell. Hemichannels can also function independently

*Corresponding author: Lilian I. Plotkin, Ph.D., Department of Anatomy and Cell Biology, Indiana University School of Medicine, 635 Barnhill Drive, MS-5035, Indianapolis, IN 46202-5120, Phone: 1-317-274-5317, Fax: 1-317-278-2040, lplotkin@iupui.edu.

of gap junctions, by mediating the exchange of small signaling molecules between the cytoplasm and the extracellular space, in bone and other tissues [10;18;19;36].

Cx43-mediated functions may be involved in cell survival or death, depending on the cell type under investigation and the intracellular pathways activated [15]. We have shown that Cx43 is required for the preservation of osteoblast and osteocyte viability by bisphosphonates *in vitro* and *in vivo* [35-37]. The carboxy terminus of Cx43 also functions as a scaffold that interacts with β -arrestin and other proteins; we have shown that this function of Cx43 is specifically required for osteoblast survival induced by parathyroid hormone (PTH) [5]. The importance of Cx43 for the response of osteocytes to pro-survival stimuli is supported by the finding that osteocytes lacking Cx43 exhibit increased apoptosis *in vitro* and *in vivo* [4]. Moreover, recent evidence indicates that osteocyte survival is critical for the maintenance of bone tissue homeostasis. In particular, osteocyte apoptosis has been suggested as the trigger for targeted bone remodeling upon immobilization, fatigue loading or ovariectomy [1;8;16].

We have previously reported that OCN-Cre;Cx43^{fl/-} mice, lacking Cx43 in osteoblasts and osteocytes [35], and DMP1-8kb-Cre;Cx43^{fl/fl} mice, lacking Cx43 only in osteocytes [4], exhibit increased prevalence of apoptosis of osteocytes, but not osteoblasts, selectively in the cortical compartment.

In this study, we investigated whether osteocyte apoptosis is also associated with decreased strength of the bone material. This connection has been previously proposed in a mouse model of glucocorticoid (GC)-induced bone loss. Specifically, in that study, the blockage of GC action selectively in osteoblasts and osteocytes protects these cells from GC-induced apoptosis and maintains the strength of the bones *in vivo* in mice [29]. Moreover, lack of Cx43 from chondro-osteoprogenitors and osteoblasts has been shown to reduce bone strength [47;49].

Here, we show that the increased apoptosis in the absence of osteocytic Cx43 is indeed accompanied by decreased stiffness of the bone material in the femoral diaphysis. Moreover, we found that Cx43 deletion in osteoblastic and osteocytic cells *in vitro* reduces the levels of lysyl oxidase, a crucial enzyme for collagen cross-linking. Thus, the decreased strength of the bone material observed *in vivo* in mice lacking Cx43 could be due to increased osteocyte apoptosis [4], consistent with a role of osteocyte survival on the maintenance of skeletal integrity, and to reduced levels of lysyl oxidase.

Materials and Methods

Mice

Mice with deletion of Cx43 from osteoblasts and osteocytes (OCN-Cre;Cx43^{fl/-}) or exclusively from osteocytes (DMP1-8kb-Cre;Cx43^{fl/fl}) were generated using the Cre/LoxP system [23;30], as previously reported [4;35]. OCN-Cre;Cx43^{fl/-} mice and Cx43^{fl/-} control littermates were generated by crossing mice homozygous for the floxed Cx43 gene (Cx43^{fl/fl} mice) [43], generated by K. Willecke, Universitat Bonn, Bonn, Germany, with Cx43^{+/-} mice [39], generated by J. Rossant, University of Toronto, ON, Canada, expressing Cre recombinase driven by the human osteocalcin promoter (OCN-Cre mice) [48], generated by T. Clemens, Johns Hopkins University School of Medicine, Baltimore, MD. This resulted in mice in a mixed C57BL/6-C129/J/FVB background. DMP1-8kb-Cre;Cx43^{fl/fl} mice and Cx43^{fl/fl} control littermates were generated by crossing Cx43^{fl/fl} mice with mice expressing Cre recombinase under an 8kb fragment of the DMP1 promoter (DMP1-8kb-Cre mice), both in a pure C57BL/6 background, previously characterized [4]. Mice were genotyped by PCR using specific primer sets [21;42;43;48]. For both mouse models, female, 4.5-month-old

mice were investigated. Mice expressing green fluorescent protein (GFP) in osteocytes (DMP1-8kb-GFP mice) were generated by I. Kalajzic, University of Connecticut Health Center, Farmington, CT [22]. All protocols involving mice were approved by the Institutional Animal Care and Use Committee of University of Arkansas for Medical Sciences and Indiana University School of Medicine.

Biomechanical testing

Three-point bending of the femur was performed at $37\pm 0.5^{\circ}\text{C}$ using a miniature bending apparatus with the posterior femoral surface lying on lower supports (7mm apart) and the left support immediately proximal to the distal condyles, as previously published [3]. The load bearing properties of the sixth lumbar vertebrae (L6) were measured using a single column material testing machine and a calibrated tension/compression load cell (Model 5542, Instron Corp., Norwood, MA), as previously described [34]. Cross-sectional moment of inertia and anterior-posterior diameter were determined by μCT and were used to calculate material-level properties, as previously described [2].

Fourier Transformed Infrared Imaging (FTIRI) data collection and analysis

FTIR imaging was performed on the vertebrae and in the cortical portion of femora. Infrared data were collected using a Spectrum Spotlight 300 FT-IR imaging system (PerkinElmer). The bone sections ($5\ \mu\text{m}$ thick) were supported between two aluminum disks (13 mm diameter \times 0.5 mm thick) each containing a narrow slit (9 mm \times 3 mm). FTIR images were collected in transmission mode from one vertebra as well as from the medial and lateral cortical shell of the mid-diaphysis of the femur from each animal, using a $6.25\ \mu\text{m}$ pixel size, 4 scans per pixel, at $8\ \text{cm}^{-1}$ spectral resolution where the background was taken through an empty section of the sample holder. Protein content was determined using the area under the amide I protein band ($1600\text{-}1700\ \text{cm}^{-1}$; baseline $1800\ \text{cm}^{-1}$). Mineral content was determined using the area under the ν_1 , ν_3 phosphate peak ($1200\text{-}900\ \text{cm}^{-1}$; baseline $1200\text{-}900\ \text{cm}^{-1}$) [17]. The level of mineralization was determined as the mineral/protein ratio to account for any variations in sample thickness. The ratio of nonreducible/reducible collagen cross-links was determined from a peak height ratio in the amide I peak ($1660/1690\ \text{cm}^{-1}$; baseline $1800\ \text{cm}^{-1}$) [32] and crystallinity was determined from a peak height ratio in the mineral phosphate peak ($1020/1030\ \text{cm}^{-1}$; baseline $1200\text{-}900\ \text{cm}^{-1}$) [27].

Micro-CT

For μCT analysis, femora were dissected, cleaned of soft tissue, fixed, and stored in 70% ethanol until imaging. Mid-diaphysis femora were scanned wrapped in parafilm using a 60kV source, 0.5 mm Al filter, 0.7 degree rotation and 2 image averaging at $6\ \mu\text{m}$ pixel resolution on the Skyscan 1172 (SkyScan, Kontich, Belgium) [6]. Reconstruction and analyses were conducted using SkyScan software. Bone was segmented from marrow for a single bone slice of the diaphysis using a similar threshold for all animals. Standard two-dimensional geometric properties, as well as bone material density in pixels, were obtained.

Cell culture

Bone marrow cells were isolated from femora and tibiae of five-month-old mice as previously published [24]. Cells were cultured in differentiation medium [α -minimal essential medium (Invitrogen) supplemented with 10% fetal bovine serum (Hyclone) and $50\ \mu\text{g/ml}$ ascorbic acid (Sigma Chemical Co.)]. After 8 days in culture, cells were harvested and RNA was extracted as described below. Osteoblastic cells were obtained from calvarial bones of neonatal mice and cultured at an initial density of $5\times 10^4/\text{cm}^2$ for 6 days in the presence of α -MEM supplemented with 10% fetal bovine serum and $50\ \mu\text{g/ml}$ ascorbic acid, as published [35]. Half of the medium was replaced by fresh medium every other day.

Osteoblastic OB-6 cells and osteocytic MLO-Y4 cells treated with scramble (scr) or Cx43 short hairpin RNA (shRNA) were cultured as previously described [4;5].

Authentic osteocyte isolation

Calvaria cells were isolated from double transgenic mice DMP1-8kb-GFP;DMP1-8kb-Cre. GFP-expressing cells (osteocyte-enriched) were separated from GFP-negative cells (osteoblast-enriched) by sorting the cell suspension using a FACSAria flow cytometer (BD Biosciences, Sparks, MD) at the Indiana University Flow Cytometry Core Facility [4].

RNA preparation and real-time PCR

Total RNA was purified using Ultraspec reagent (Biotecx Laboratories) and Taqman quantitative RT-PCR was performed, as previously described [35]. Primers and probes for floxed-Cx43 and CRE recombinase were manufactured by the Assays-by-Design service from Applied Biosystems (Life Technologies Corp.). Primers for *Lox* and *Lox1* 1-4 were designed using the assay design center (Roche Applied Science). Relative mRNA expression levels were obtained by normalizing to the house-keeping gene mitochondrial ribosomal protein S2 (*Mrps2*) or glyceraldehyde 3-phosphate dehydrogenase (*GAPDH*) (Applied Biosystems) using the ΔC_t method [25].

Statistical analysis

Significance was evaluated by t-test using SigmaStat (SPSS Science). For FTIRI, Independent Mann Whitney U-tests were performed because it is a non-parametric statistical approach for testing for significance between small groups without the assumption of normally (Gaussian) distributed data. Differences were considered significant for $p < 0.05$.

Results

Material stiffness is decreased in femoral bone of OCN-Cre;Cx43^{fl/-} and DMP1-8kb-Cre;Cx43^{fl/fl} mice

We have previously shown that OCN-Cre;Cx43^{fl/-} mice (lacking Cx43 in osteoblasts and osteocytes) and DMP1-8kb-Cre;Cx43^{fl/fl} mice (lacking Cx43 only in osteocytes) display high osteocyte apoptosis only in the cortical envelope of the vertebrae and in the diaphysis of femora [4]. Increased osteocyte death was associated with changes in bone geometry at the femoral midshaft, but not in the microarchitecture of cancellous bone in the distal femur metaphysis. Three-point bending of the femur was used to obtain the biomechanical properties of the bones in the two mouse models. Three-point bending showed that stiffness and ultimate load were not different between OCN-Cre;Cx43^{fl/-} and control mice (Fig. 1A), although the femoral midshaft of OCN-Cre;Cx43^{fl/-} mice has higher moment of inertia compared to control animals, due to widening of the cross-section, as previously shown [4]. Stiffness and ultimate load are also called “extrinsic” parameters, because they depend on the size and shape of the bone [44]. Therefore, we determined the “intrinsic” strength values, to understand whether the benefit given by the geometry was canceled out by a poor quality of the bone material, which also contributes to the overall resistance of the bone to bending. To do this, we applied engineering formulas [45] that correct the “extrinsic” parameters by the geometry of the femoral cross-section to obtain the strength and stiffness per unit of area. We found that OCN-Cre;Cx43^{fl/-} mice displayed a 25% lower material stiffness (Young's modulus) and a lower, although not significant ($P=0.055$), ultimate stress (Fig. 1A). This indicates that the lower bone material quality in OCN-Cre;Cx43^{fl/-} mice mechanically offsets the beneficial geometrical adaptation of the femora. Similarly, femoral mechanical strength was not improved in DMP1-8kb-Cre;Cx43^{fl/fl} mice, despite the higher moment of inertia, due to a reduced quality of the bone material. Indeed, DMP1-8kb-

Cre;Cx43^{fl/fl} mice exhibited a marked reduction in material properties, as Young's modulus was decreased by approximately 50% and ultimate stress was significantly lower than in control animals (Fig. 1B). Thus, Cx43 deletion in both animal models reduces the strength of the material in cortical bone.

OCN-Cre;Cx43^{fl/-} and DMP1-8kb-Cre;Cx43^{fl/fl} mice do not exhibit common changes in microscopic material properties assessed by FTIR

Young's modulus is determined by the degree of mineralization, as well as by the composition of the organic matrix [7]. We therefore analyzed the properties of the bone matrix in OCN-Cre;Cx43^{fl/-} mice by FTIRI in the appendicular skeleton (left femur, only cortical bone). A small, non-significant decrease in mineralization was observed in OCN-Cre;Cx43^{fl/-} mice compared to control littermates (Fig. 2A). The ratio of nonreducible/reducible cross-links was selectively decreased in femoral cortical bone of OCN-Cre;Cx43^{fl/-} mice compared to control mice. On the other hand, in DMP1-8kb-Cre;Cx43^{fl/fl} mice collagen maturation was not different compared to control animals, while mineralization was significantly, although slightly, reduced in the femoral diaphysis (Fig. 2B). No differences were found in any parameter in cancellous bone of distal femur between the DMP1-8kb-Cre;Cx43^{fl/fl} and control mice. Mineralization and collagen cross-linking was higher in the femoral cortex compared to the cancellous bone in the femoral metaphysis, independently of the genotype under consideration. μ CT analysis showed no change in cortical bone material density in OCN-Cre;Cx43^{fl/-} or DMP1-8kb-Cre;Cx43^{fl/fl} mice compared to controls (Fig. 2C), in spite of the decrease in mineralization detected by FTIRI in DMP1-8kb-Cre;Cx43^{fl/fl} mice.

Deletion of Cx43 from osteoblastic cells does not affect vertebral bone

Consistent with the lack of a phenotypic effect in trabecular bone, compression measurements of bone strength on the lumbar vertebra L5, which is mainly composed of cancellous bone, showed that the mechanical parameter ultimate load was not affected by Cx43 deletion in OCN-Cre;Cx43^{fl/-} mice (Fig. 3A). Moreover, strength/unit of area, determined by correcting this measurement by the cross-sectional area of the vertebral body, was not different between genotypes. Thus, in bones where strength is mainly determined by the cancellous compartment, both mechanical and material strengths were not affected by the lack of Cx43. Moreover, there was no difference between control and OCN-Cre;Cx43^{fl/-} mice in any parameter (mineralization, cristallinity, collagen cross-linking) in the cancellous or cortical bone of the vertebrae (Fig. 3B). Mineralization, expressed as the ratio phosphate/protein, was significantly higher in the cortical compartment of the femur compared to the same compartment in the vertebra, independently of the genotype (Fig. 2B and 3B). On the other hand cristallinity, which is a measure of crystal size and maturation, was lower in the cortical bone of the femur compared to the vertebral cortex in Cx43^{fl/-} mice. Collagen cross-linking did not differ between cancellous and cortical compartments in the vertebrae or between axial and appendicular skeleton.

Cx43 removal reduces the expression of lysyl oxidase (Lox) in osteoblastic and osteocytic cell lines in a cell autonomous manner

The formation of collagen cross-links is initiated by conversion of lysyl or hydroxylysyl residues, present in collagen telopeptides, to aldehydes catalyzed by lysyl oxidases (Lox) [40;46]. This first step is followed by condensation with adjacent Lys or Hyl, to give immature, reducible cross-links [40]. Therefore, the decrease in the non-reducible/reducible crosslinks ratio could be due to lower levels of lysyl oxidase in Cx43-deficient animals compared to controls. The main form of lysyl oxidase is Lox; there are also 4 additional isoforms called Lox-like (Loxl) 1-4 [33]. First, we evaluated the expression levels of the different isoforms of lysyl oxidase in authentic osteoblasts and osteocytes. To do this, we

used RNA from calvaria cells isolated from DMP1-GFP mice. In these mice osteocytes are labeled with GFP, while osteoblasts are GFP negative, thus allowing their separation by Fluorescence Activated Cell Sorting [22]. We have previously shown that the GFP-positive fraction exhibits gene expression consistent with osteocytic cells, i.e.: reduced levels of keratocan (a gene enriched in osteoblasts) and high expression of the osteocyte-specific gene sclerostin [4]. The GFP-negative fraction on the other hand, expresses high levels of keratocan and lacks sclerostin, consistent with osteoblastic cells. We found that *Lox* was the most abundant lysyl oxidase in both cell types. The expression of *Lox* and *Loxl-1* was 7 and 2 times higher in osteoblasts compared to osteocytes respectively, whereas *Loxl-3* and *Loxl-4* were comparable in the two cell types and were at least 10 times lower than *Loxl-1*, while *Loxl-2* could not be detected (Fig. 4A). These findings were confirmed in RNA purified from tibia diaphysis of 16 week-old wild type C57BL/6 mice (Fig. 4B). Therefore, we focused our attention on *Lox* and *Loxl-1*, since they are the main forms of *Lox* expressed by bone cells. We measured the levels of *Lox* and *Loxl-1* in primary calvaria cells isolated from OCN-Cre;*Cx43*^{fl/-} and DMP1-8kb-Cre;*Cx43*^{fl/fl} mice and the respective control littermates and grown for 7 days in the presence of differentiation media. *Cx43* was decreased in both primary calvaria cell preparations, although significantly only in cells isolated from DMP1-8kb-Cre;*Cx43*^{fl/fl} mice (Fig. 4C). We found that the levels of *Lox* and *Loxl-1* did not change significantly in response of lack of *Cx43* in either culture. To determine whether deletion of *Cx43* could have a cell autonomous effect on *Lox/Loxl-1* expression levels we evaluated their levels in osteoblastic OB-6 cells and in osteocytic MLO-Y4 cells, in which *Cx43* expression was silenced by shRNA [4;5]. We found that both osteoblasts and osteocytes with reduced *Cx43* exhibit decreased *Lox* and increased *Loxl-1* (Fig. 4D). Consistent with the relative levels of *Lox* and *Loxl-1* in primary osteoblasts and osteocytes (Fig. 4A), the enzymes were more abundant in osteoblastic cells, compared to osteocytes. These findings suggest that *Lox* and *Loxl-1* transcription or mRNA stability is affected by deletion of *Cx43* in osteoblastic cells.

Discussion

We have previously shown that *Cx43* deletion from osteoblasts and osteocytes or only from osteocytes results in increased cortical osteocyte apoptosis and widening of the femoral cross-sections. We report herein that both mouse models of *Cx43* deletion also exhibit decreased bone material properties selectively in cortical bone. Two recent reports also show widening of the marrow cavity and periosteal expansion in growing (1-2 month-old) mice with deletion of *Cx43* from chondro-osteoprogenitors using the *dermo1* promoter [47] or from osteoblasts/osteocytes using the OCN-Cre transgene (the same model used in our studies) [49]. However, unlike our study, these reports show decreased bone mass and mechanical properties in the femoral midshaft. In particular, deletion of *Cx43* from chondro-osteoprogenitors results in a strong phenotype, with decreased BMD, femoral length and an approximately 50% decrease in yield force [47]. Similarly, Zhang et al. reported that OCN-Cre;*Cx43*^{fl/fl} mice exhibit decreased BMD and mechanical and material properties in the femoral midshaft [49]. On the other hand, in the current study we did not find changes in mechanical properties when *Cx43* was deleted from osteoblasts/osteocytes or from osteocytes. This apparent discrepancy could be explained by the fact that our study was performed in adult (4.5-month-old) mice in which the growth of the femoral bone might have offset the deficient material properties, resulting in unaltered mechanical strength. Moreover, our data showing that DMP1-8kb-Cre;*Cx43*^{fl/fl} mice exhibit a similar decrease in material properties to OCN-Cre;*Cx43*^{fl/fl} mice, reported by Zhang et al [49] and by us (this report), indicate that osteocytes contribute to the maintenance of the strength of the bone material. This finding points to a higher complexity of osteocytic tasks than what previously thought and it is in line with a recent report showing that osteocytes can also exert typical osteoclastic functions, such as dissolution of matrix and mineral around their lacunae [38].

Mechanical testing shows phenotypic differences between Cx43^{fl/-} and Cx43^{fl/fl} control mice, which could be due to the Cx43 haploinsufficiency in the first model or to the different genetic backgrounds of the two mouse models (mixed C57BL/6-C129/J/FVB and pure C57BL/6 background for Cx43^{fl/-} and Cx43^{fl/fl} mice, respectively). Nevertheless, in the femora, the lack of Cx43 in both models significantly decreased Young's modulus, which is a measure of the rigidity or stiffness of the bone material that is determined by the amount of mineral and, to a lesser extent, by collagen [7]. However, mineralization measured by μ CT was not different between the two genotypes, and it was only slightly, but significantly reduced in the DMP1-8kb-Cre;Cx43^{fl/fl} mice as assessed by FTIRI. Although the decrease in mineralization appeared to be very small, several studies have demonstrated that even a very small increase in mineral volume fraction will have a very large effect on modulus [12;13;26;31]. The finding that mineralization is not reduced in OCN-Cre;Cx43^{fl/fl} mice suggests that, besides mineralization, other properties of the bone material contribute to the reduction in Young's modulus in both animal models. Moreover, the reduction in mineralization might occur in spatially restricted areas of the cortical bone, likely associated to osteocyte apoptosis and remodeling, thus increasing the variability of the mineralization measurements and decreasing the difference between genotypes. Future studies will evaluate whether changes in bone material properties correlate with areas with increased osteocyte apoptosis.

Collagen cross-linking is an important determinant of bone biomechanical properties [9;14] and could explain at least part of the decrease in bone material properties. During collagen maturation the content of reducible cross-links diminishes whereas that of non-reducible cross-links increases, because with time the former likely matures into the latter [32]. Our FTIRI findings that the ratio of non-reducible/reducible cross-links decreases in OCN-Cre;Cx43^{fl/-} mice suggest that the lack of Cx43 hampers the proper maturation of collagen cross-links. Moreover, altered bone matrix with disorganized collagen fibers was also reported in mice lacking Cx43 early in the chondro-osteogenic lineage, in which osteoblast differentiation/function and lysyl oxidase levels are markedly reduced [47]. Although DMP1-8kb-Cre;Cx43^{fl/fl} mice also display a marked decrease in the strength of the bone material at the femoral diaphysis, we could not detect a significant decrease in collagen cross-linking by FTIRI. However, Cx43 down-regulation lowers the levels of Lox and Lox1-1 in osteoblastic and osteocytic cell lines, indicating that Cx43 may be required in a cell autonomous manner for the expression of these enzymes in both cell types. Whether the modulation of Lox occurs through mRNA stabilization or active promotion of transcription by Cx43 is not known. We speculate that the effect of Cx43 deletion in osteoblasts, which express higher levels of Lox and Lox1-1 as shown by 10-times higher levels of Lox in OB-6 osteoblastic cells, compared to MLO-Y4 osteocytic cells (Fig. 4C), has more dramatic consequences for bone and that the expression of lysyl oxidase in osteocytes is less crucial for collagen cross-linking. In addition, the lack of a reduction in Lox in calvaria cells isolated from the two mouse models points to the intriguing possibility that the decrease in Lox is a phenotypic feature exclusively of cortical bone of the appendicular skeleton and may be absent in other skeletal sites, such as the skull.

Some of the material properties we assessed by FTIRI were found to vary in different bone compartments and skeletal sites. Cortical bone of the femoral diaphysis had higher mineralization compared to cortical or cancellous bone of the vertebra and to cancellous bone of the femur itself. This could indicate that bone in the femoral cortex is deposited earlier and does not get remodeled as much as the cancellous bone, due to the lower rate of bone remodeling of cortical bone.

As reported in a previous publication of ours [4], bones from OCN-Cre;Cx43^{fl/-} and DMP1-8kb-Cre;Cx43^{fl/fl} mice exhibit features that are found in aged subjects, including

increased osteocyte apoptosis and widening of the femoral cross-section. Remarkably, with age, both the enzymatic crosslinks [41] and the activity of Lox appear to decline [28], thus further indicating that the loss of Cx43 accelerates the appearance of features of aging in bone. Further studies will be conducted to shed light into the contribution of reduced Cx43 expression to the aging of bone tissue.

In summary, although osteoblasts are likely to be the primary responsible cells for manufacturing matrix, our data point to a contribution of osteocytes to the regulation of the quality of the bone material. Moreover, Cx43 expression in both osteoblasts and osteocytes is important for maintaining the stiffness of the bone material, but the mechanism might be different in osteocytes where it might depend also on Cx43-mediated control of osteocyte viability.

Acknowledgments

The authors thank Kanan Vyas, Drs. Keith Condon and Ignacio Aguirre for technical assistance and Drs. Charles Tuner, David Burr, and Matthew Allen for insightful suggestions. This research was supported by the National Institutes of Health (R01-AR053643). μ CT studies were performed using equipment obtained with the NIH grant S10-RR023710 (PI: James Williams, Department of Anatomy and Cell Biology, Indiana University School of Medicine).

References

1. Aguirre JI, Plotkin LI, Stewart SA, Weinstein RS, Parfitt AM, Manolagas SC, Bellido T. Osteocyte apoptosis is induced by weightlessness in mice and precedes osteoclast recruitment and bone loss. *J Bone Min Res.* 2006; 21:605–615.
2. Allen MR, Reinwald S, Burr DB. Alendronate reduces bone toughness of ribs without significantly increasing microdamage accumulation in dogs following 3 years of daily treatment. *Calcif Tissue Int.* 2008; 82:354–360. [PubMed: 18463913]
3. Almeida M, Han L, Martin-Millan M, Plotkin LI, Stewart SA, Roberson PK, Kousteni S, O'Brien CA, Bellido T, Parfitt AM, Weinstein RS, Jilka RL, Manolagas SC. Skeletal involution by age-associated oxidative stress and its acceleration by loss of sex steroids. *J Biol Chem.* 2007; 282:27285–27297. [PubMed: 17623659]
4. Bivi N, Condon KW, Allen MR, Farlow N, Passeri G, Brun L, Rhee Y, Bellido T, Plotkin LI. Cell autonomous requirement of connexin 43 for osteocyte survival: consequences for endocortical resorption and periosteal bone formation. *J Bone Min Res.* 2012; 27:374–389.
5. Bivi N, Lezcano V, Romanello M, Bellido T, Plotkin LI. Connexin43 interacts with parrestin: a prerequisite for osteoblast survival induced by parathyroid hormone. *J Cell Biochem.* 2011; 112:2920–2930. [PubMed: 21630325]
6. Bouxsein ML, Boyd SK, Christiansen BA, Guldberg RE, Jepsen KJ, Muller R. Guidelines for assessment of bone microstructure in rodents using micro-computed tomography. *J Bone Miner Res.* 2010; 25:1468–1486. [PubMed: 20533309]
7. Burr DB. The contribution of the organic matrix to bone's material properties. *Bone.* 2002; 31:8–11. [PubMed: 12110405]
8. Cardoso L, Herman BC, Verborgt O, Laudier D, Majeska RJ, Schaffler MB. Osteocyte apoptosis controls activation of intracortical resorption in response to bone fatigue. *J Bone Miner Res.* 2009; 24:597–605. [PubMed: 19049324]
9. Chavassieux P, Seeman E, Delmas PD. Insights into material and structural basis of bone fragility from diseases associated with fractures: how determinants of the biomechanical properties of bone are compromised by disease. *Endocr Rev.* 2007; 28:151–164. [PubMed: 17200084]
10. Cherian PP, Siller-Jackson AJ, Gu S, Wang X, Bonewald LF, Sprague E, Jiang JX. Mechanical strain opens connexin 43 hemichannels in osteocytes: a novel mechanism for the release of prostaglandin. *Mol Biol Cell.* 2005; 16:3100–3106. [PubMed: 15843434]
11. Civitelli R. Cell-cell communication in the osteoblast/osteocyte lineage. *Arch Biochem Biophys.* 2008; 473:188–192. [PubMed: 18424255]

12. Currey JD. The mechanical consequences of variation in the mineral content of bone. *J Biomech.* 1969; 2:1–11. [PubMed: 16335107]
13. Currey JD. The relationship between the stiffness and the mineral content of bone. *J Biomech.* 1969; 2:477–480. [PubMed: 16335147]
14. Davison KS, Siminoski K, Adachi JD, Hanley DA, Goltzman D, Hodzman AB, Josse R, Kaiser S, Olszynski WP, Papaioannou A, Ste-Marie LG, Kendler DL, Tenenhouse A, Brown JP. Bone strength: the whole is greater than the sum of its parts. *Semin Arthritis Rheum.* 2006; 36:22–31. [PubMed: 16887465]
15. Decrock E, Vinken M, De Vuyst E, Krysko DV, D'Herde K, Vanhaecke T, Vandennebeele P, Rogiers V, Leybaert L. Connexin-related signaling in cell death: to live or let die? *Cell Death Differ.* 2009; 16:524–536. [PubMed: 19197295]
16. Emerton KB, Hu B, Woo AA, Sinofsky A, Hernandez C, Majeska RJ, Jepsen KJ, Schaffler MB. Osteocyte apoptosis and control of bone resorption following ovariectomy in mice. *Bone.* 2009; 46:577–583. [PubMed: 19925896]
17. Gadaleta SJ, Paschalis EP, Betts F, Mendelsohn R, Boskey AL. Fourier transform infrared spectroscopy of the solution-mediated conversion of amorphous calcium phosphate to hydroxyapatite: new correlations between X-ray diffraction and infrared data. *Calcif Tissue Int.* 1996; 58:9–16. [PubMed: 8825233]
18. Genetos DC, Kephart CJ, Zhang Y, Yellowley CE, Donahue HJ. Oscillating fluid flow activation of gap junction hemichannels induces ATP release from MLO-Y4 osteocytes. *J Cell Physiol.* 2007; 212:207–214. [PubMed: 17301958]
19. Goodenough DA, Paul DL. Beyond the gap: functions of unpaired connexon channels. *Nat Rev Mol Cell Biol.* 2003; 4:285–294. [PubMed: 12671651]
20. Goodenough DA, Paul DL. Gap junctions. *Cold Spring Harb Perspect Biol.* 2009; 1:a002576. [PubMed: 20066080]
21. Hilton MJ, Tu X, Wu X, Bai S, Zhao H, Kobayashi T, Kronenberg HM, Teitelbaum SL, Ross FP, Kopan R, Long F. Notch signaling maintains bone marrow mesenchymal progenitors by suppressing osteoblast differentiation. *Nat Med.* 2008; 14:306–314. [PubMed: 18297083]
22. Kalajzic I, Braut A, Guo D, Jiang X, Kronenberg MS, Mina M, Harris MA, Harris SE, Rowe DW. Dentin matrix protein 1 expression during osteoblastic differentiation, generation of an osteocyte GFP-transgene. *Bone.* 2004; 35:74–82. [PubMed: 15207743]
23. Lakso M, Sauer B, Mosinger B Jr, Lee EJ, Manning RW, Yu SH, Mulder KL, Westphal H. Targeted oncogene activation by site-specific recombination in transgenic mice. *Proc Natl Acad Sci U S A.* 1992; 89:6232–6236. [PubMed: 1631115]
24. Lecka-Czernik B, Gubrij I, Moerman EA, Kajkenova O, Lipschitz DA, Manolagas SC, Jilka RL. Inhibition of *Osf2/Cbfa1* expression and terminal osteoblast differentiation by PPAR-gamma 2. *J Cell Biochem.* 1999; 74:357–371. [PubMed: 10412038]
25. Livak KJ, Schmittgen TD. Analysis of relative gene expression data using real-time quantitative PCR and the $2^{-\Delta\Delta CT}$ method. *Methods.* 2001; 25:402–408. [PubMed: 11846609]
26. Miller LM, Little W, Schirmer A, Sheik F, Busa B, Judex S. Accretion of bone quantity and quality in the developing mouse skeleton. *J Bone Miner Res.* 2007; 22:1037–1045. [PubMed: 17402847]
27. Miller LM, Vairavamurthy V, Chance MR, Mendelsohn R, Paschalis EP, Betts F, Boskey AL. In situ analysis of mineral content and crystallinity in bone using infrared micro-spectroscopy of the $\nu(4) PO(4)(3-)$ vibration. *Biochim Biophys Acta.* 2001; 1527:11–19. [PubMed: 11420138]
28. Nyman JS, Roy A, Acuna RL, Gayle HJ, Reyes MJ, Tyler JH, Dean DD, Wang X. Age-related effect on the concentration of collagen crosslinks in human osteonal and interstitial bone tissue. *Bone.* 2006; 39:1210–1217. [PubMed: 16962838]
29. O'Brien CA, Jia D, Plotkin LI, Bellido T, Powers CC, Stewart SA, Manolagas SC, Weinstein RS. Glucocorticoids act directly on osteoblasts and osteocytes to induce their apoptosis and reduce bone formation and strength. *Endocrinology.* 2004; 145:1835–1841. [PubMed: 14691012]
30. Orban PC, Chui D, Marth JD. Tissue- and site-specific DNA recombination in transgenic mice. *Proc Natl Acad Sci U S A.* 1992; 89:6861–6865. [PubMed: 1495975]

31. Paschalis EP, Tatakis DN, Robins S, Fratzl P, Manjubala I, Zoehrer R, Gamsjaeger S, Buchinger B, Roschger A, Phipps R, Boskey AL, Dall'Ara E, Varga P, Zysset P, Klaushofer K, Roschger P. Lathyrisms-induced alterations in collagen cross-links influence the mechanical properties of bone material without affecting the mineral. *Bone*. 2011; 49:1232–1241. [PubMed: 21920485]
32. Paschalis EP, Verdelis K, Doty SB, Boskey AL, Mendelsohn R, Yamauchi M. Spectroscopic characterization of collagen cross-links in bone. *J Bone Miner Res*. 2001; 16:1821–1828. [PubMed: 11585346]
33. Pischon N, Maki JM, Weisshaupt P, Heng N, Palamakumbura AH, N'Guessan P, Ding A, Radlanski R, Renz H, Bronckers TA, Myllyharju J, Kielbassa AM, Kleber BM, Bernimoulin JP, Trackman PC. Lysyl oxidase (lox) gene deficiency affects osteoblastic phenotype. *Calcif Tissue Int*. 2009; 85:119–126. [PubMed: 19458888]
34. Plotkin LI, Bivi N, Bellido T. A bisphosphonate that does not affect osteoclasts prevents osteoblast and osteocyte apoptosis and the loss of bone strength induced by glucocorticoids in mice. *Bone*. 2011; 49:122–127. [PubMed: 20736091]
35. Plotkin LI, Lezcano V, Thostenson J, Weinstein RS, Manolagas SC, Bellido T. Connexin 43 is required for the anti-apoptotic effect of bisphosphonates on osteocytes and osteoblasts in vivo. *J Bone Miner Res*. 2008; 23:1712–1721. [PubMed: 18597631]
36. Plotkin LI, Manolagas SC, Bellido T. Transduction of cell survival signals by connexin-43 hemichannels. *J Biol Chem*. 2002; 277:8648–8657. [PubMed: 11741942]
37. Plotkin LI, Weinstein RS, Parfitt AM, Roberson PK, Manolagas SC, Bellido T. Prevention of osteocyte and osteoblast apoptosis by bisphosphonates and calcitonin. *J Clin Invest*. 1999; 104:1363–1374. [PubMed: 10562298]
38. Qing H, Ardeshirpour L, Pajevic PD, Dusevich V, Jahn K, Kato S, Wysolmerski J, Bonewald LF. Demonstration of osteocytic perilacunar/canalicular remodeling in mice during lactation. *J Bone Miner Res*. 2012; 27:1018–1029. [PubMed: 22308018]
39. Reaume AG, de Sousa PA, Kulkarni S, Langille BL, Zhu D, Davies TC, Juneja SC, Kidder GM, Rossant J. Cardiac malformation in neonatal mice lacking connexin43. *Science*. 1995; 267:1831–1834. [PubMed: 7892609]
40. Saito M, Marumo K. Collagen cross-links as a determinant of bone quality: a possible explanation for bone fragility in aging, osteoporosis, and diabetes mellitus. *Osteoporos Int*. 2010; 21:195–214. [PubMed: 19760059]
41. Sanada H, Shikata J, Hamamoto H, Ueba Y, Yamamuro T, Takeda T. Changes in collagen cross-linking and lysyl oxidase by estrogen. *Biochim Biophys Acta*. 1978; 541:408–413. [PubMed: 27234]
42. Silverstein DM, Urban M, Gao Y, Mattoo TK, Spray DC, Rozental R. Renal morphology in connexin43 knockout mice. *Pediatr Nephrol*. 2001; 16:467–471. [PubMed: 11420908]
43. Theis M, de Wit C, Schlaeger TM, Eckardt D, Kruger O, Doring B, Risau W, Deutsch U, Pohl U, Willecke K. Endothelium-specific replacement of the connexin43 coding region by a lacZ reporter gene. *Genesis*. 2001; 29:1–13. [PubMed: 11135457]
44. Turner CH. Bone strength: current concepts. *Ann NY Acad Sci*. 2006; 1068:429–446. [PubMed: 16831941]
45. Turner CH, Burr DB. Basic biomechanical measurements of bone: a tutorial. *Bone*. 1993; 14:595–608. [PubMed: 8274302]
46. Viguet-Carrin S, Garnero P, Delmas PD. The role of collagen in bone strength. *Osteoporos Int*. 2006; 17:319–336. [PubMed: 16341622]
47. Watkins M, Grimston SK, Norris JY, Guillotin B, Shaw A, Beniash E, Civitelli R. Osteoblast Connexin43 modulates skeletal architecture by regulating both arms of bone remodeling. *Mol Biol Cell*. 2011; 22:1240–1251. [PubMed: 21346198]
48. Zhang M, Xuan S, Bouxsein ML, Von Stechow D, Akeno N, Faugere MC, Malluche H, Zhao G, Rosen CJ, Efstratiadis A, Clemens TL. Osteoblast-specific knockout of the insulin-like growth factor (IGF) receptor gene reveals an essential role of IGF signaling in bone matrix mineralization. *J Biol Chem*. 2002; 277:44005–44012. [PubMed: 12215457]

49. Zhang Y, Paul EM, Sathyendra V, Davidson A, Bronson S, Srinivasan S, Gross TS, Donahue HJ. Enhanced osteoclastic resorption and responsiveness to mechanical load in gap junction deficient bone. PLoS ONE. 2011; 6:e23516. [PubMed: 21897843]

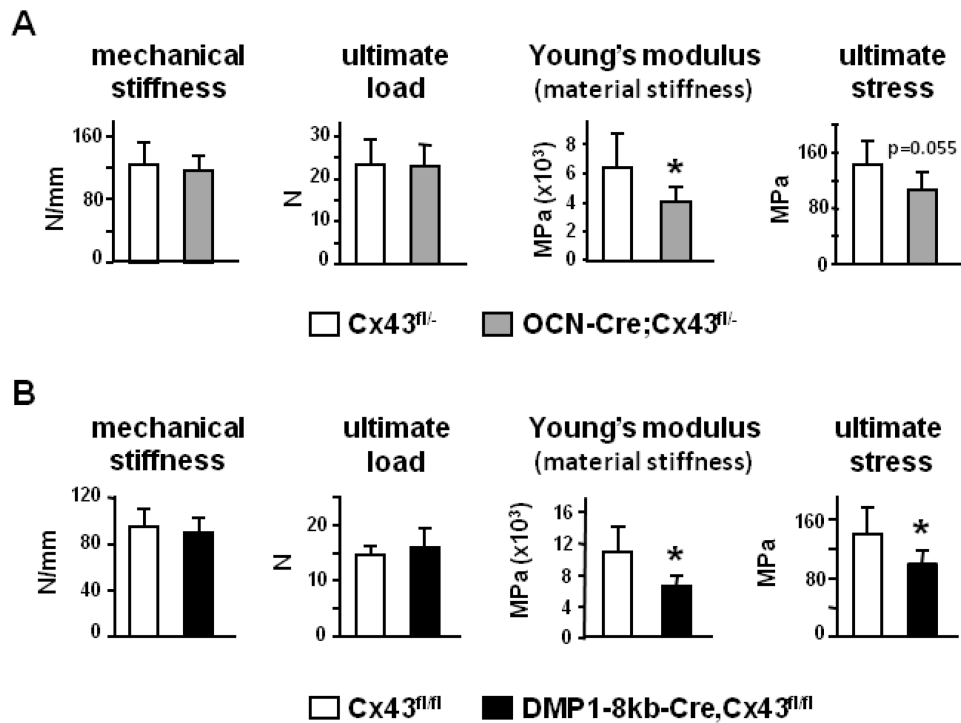


Figure 1. OCN-Cre;Cx43^{fl/-} and DMP1-8kb-Cre;Cx43^{fl/fl} mice have decreased material properties in the femur

Mechanical properties of the femur from Cx43^{fl/-} and OCN-Cre;Cx43^{fl/-} mice (A) and Cx43^{fl/fl} and DMP1-8kb-Cre;Cx43^{fl/fl} mice (B) were determined by 3-point bending. Bars are mean \pm SD. *, indicates significant pairwise differences at $p < 0.05$, $n = 6-11$.

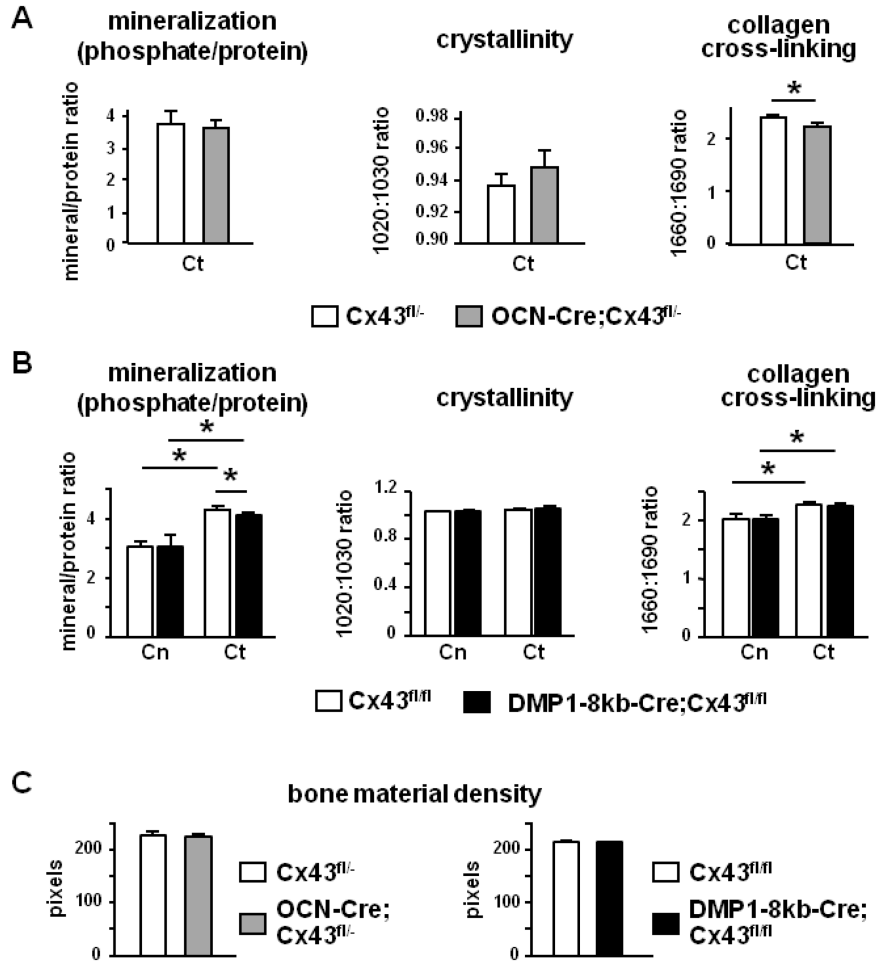


Figure 2. Deletion of Cx43 from osteoblasts and osteocytes results in reduced maturation of collagen cross-links in the femoral midshaft

Bone mineralization, crystallinity and collagen cross-linking were assessed in the femora by FTIRI in (A) cortical compartment of the diaphysis of Cx43^{fl/-} and OCN-Cre;Cx43^{fl/-} mice and (B) cancellous compartment of distal femora and cortical compartment of the diaphysis of Cx43^{fl/fl} and DMP1-8kb-Cre;Cx43^{fl/fl} mice. Ct: cortical, Cn: cancellous. Bars are mean ± SD. *, p<0.05 by independent Mann Whitney u-tests, n= 3. (C) Bone material density was measured by μCT in the femoral midshaft. Bars are mean ± SD, n=7-10.

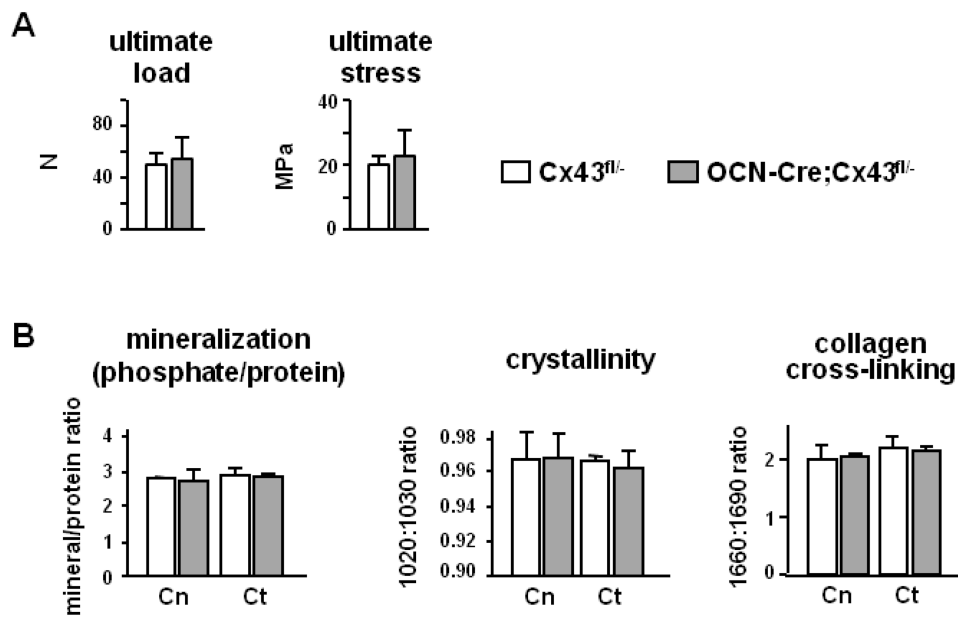


Figure 3. Deletion of Cx43 from osteoblasts and osteocytes does not affect vertebral bone (A) Mechanical properties of the lumbar vertebra L5 from Cx43^{fl/-} and OCN-Cre;Cx43^{fl/-} mice were determined by vertebral compression. Bars are mean ± SD. n = 6-11. (B) Bone mineralization, crystallinity and collagen cross-linking were assessed by FTIRI in the cancellous and cortical compartments of lumbar vertebra L5. Bars are mean ± SD, n= 3.

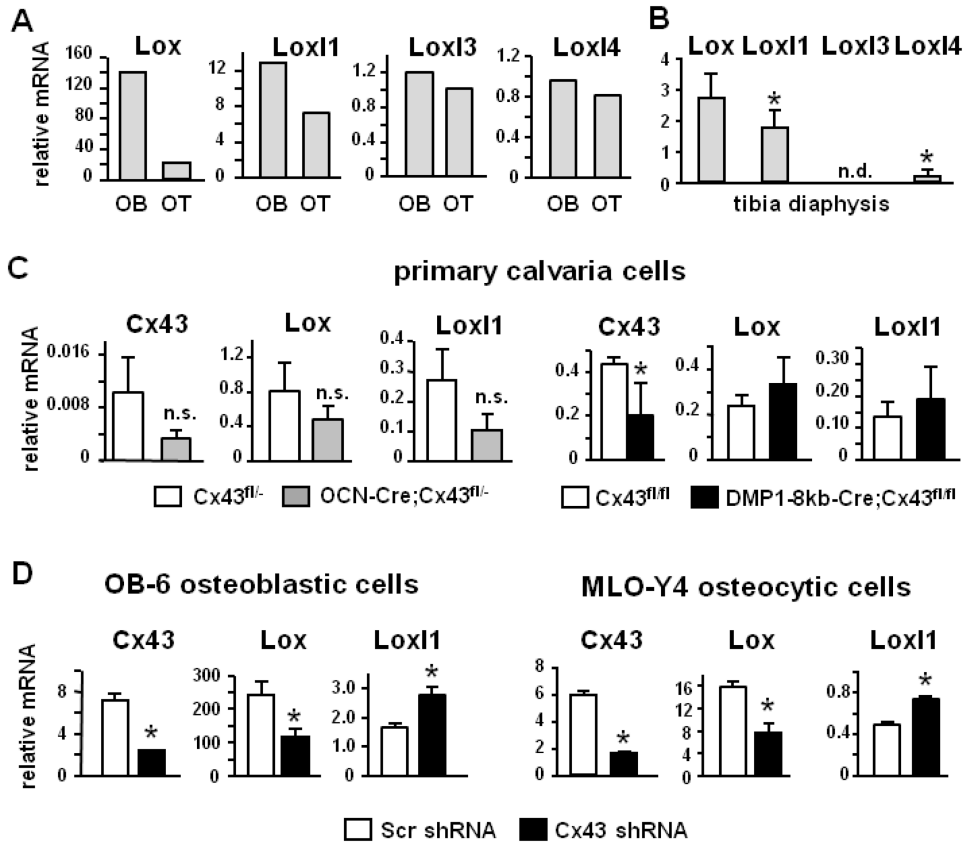


Figure 4. Deletion of Cx43 results in decreased expression of Lox
(A) mRNA levels of the indicated genes in calvaria cells isolated from the progeny of DMP1-GFP;DMP1-8kb-Cre separated by FACS in GFP-negative and GFP-positive fractions. Mrsp2 was used as housekeeping gene. OB: osteoblasts; OT: osteocytes. **(B)** mRNA levels of the indicated genes in RNA purified from tibia diaphysis from wild type C57BL/6 mice. Mrsp2 was used as housekeeping gene. Bars are mean \pm SD. *, indicates significant differences at $p < 0.05$ vs Lox levels, $n = 6$. **(C)** Expression levels of Cx43, Lox, and Lox1-1 in primary calvaria cells from Cx43^{fl/-} and OCN-Cre;Cx43^{fl/-} mice and Cx43^{fl/fl} and DMP1-8kb-Cre;Cx43^{fl/fl} mice after 7 days in culture with ascorbic acid to induce differentiation into the osteogenic lineage. Data are expressed as relative to Mrsp2. Bars are mean \pm SD. n.s. indicates not significant. **(D)** Expression levels of Cx43, Lox, and Lox1-1 in osteoblastic OB-6 cells and osteocytic MLO-Y4 cells with (scr shRNA) and without Cx43 (Cx43 shRNA). Data are expressed as relative to Mrsp2. Bars are mean \pm SD. *, indicates significant differences at $p < 0.05$, $n = 3$.